I&EC research
Industrial & Engineering Chemistry Research

Article

pubs.acs.org/IECR

Monolithic Stirrer Reactor: Performance in the Partial Hydrogenation of Sunflower Oil

Diego E. Boldrini, Jhon F. Sánchez M., Gabriela M. Tonetto,* and Daniel E. Damiani

Planta Piloto de Ingeniería Química PLAPIQUI (UNS−CONICET), Camino "La Carrindanga" Km 7, CC 717, CP 8000, Bahía Blanca, Argentina

ABSTRACT: In the present paper, the performance of monolithic catalysts obtained from a catalytic converter was analyzed in the partial hydrogenation of sunflower oil. The monoliths were reimpregnated with palladium and installed as a blade in a monolithic stirrer reactor. The use of this type of reactor was explored in the reaction at 373 K and 413 kPa, analyzing the effect variables such as stirrer speed, hydrogen supply, and stirrer design on the catalyst activity and selectivity to trans-isomers and saturated product. The volumetric gas−liquid and liquid−solid mass transfer coefficients were calculated, and the influence of the stirrer speed was examined. Estimations of the Carberry numbers and Weisz−Prater modulus were used for establishing the presence or absence of mass transfer resistances. The performance of the catalyst was studied in consecutive tests, and different procedures for catalyst regeneration were applied.

1. INTRODUCTION

Monolithic catalysts are extensively used in environmentally related gas-phase reactions. They have been mainly used for automobile exhaust emissions control, although they are progressively used in other industrial applications. The multichannel structure of those used for car emissions control is made of cordierite ($2MgO{\cdot}2Al_2O_3{\cdot}5SiO_2$). The active phase of the catalyst (Pt, Pd, Rh) is dispersed on an alumina support on top of the cordierite matrix. Cordierite monoliths present several advantages. They resist high temperatures and thermal and mechanical shocks and they have a low thermal expansion coefficient. These properties make them suitable for industrial applications.

Monolithic reactors allow for better flow conditions, lower pressure drop, high area/volume ratio and mechanical resistance. However, some disadvantages also exist.

The variety of materials and technologies available for preparation of monolithic catalysts make it possible to use these structures in reactors of various configurations: in flow reactors, in tank reactors, in recirculating reactors, with oscillation, with jets, with flow distributors, with different flow impellers, etc.[1,2] In principle, all of these new technologies are applicable to oil hydrogenation, the goal of this work, probably implying important modifications to the present industrial process. An easier design to implement is the monolithic stirrer reactor.

Carberry[3] was the first to introduce the idea of including the catalyst in the agitation device of a tank reactor. His invention was named the spinning basket gradientless reactor and was used for kinetic studies without external mass transfer limitations. In 1994, Kolaczkowski[4] introduced a spinning reactor including pieces of a monolithic catalyst in the basket. A short time later, based on a previous work of Bennet et al.,[5] Edvinson et al.[6] proposed the use of a tank reactor having monolithic catalyst blocks in the agitator. A tank reactor where the impeller blades are replaced by monolithic catalyst is referred to as a monolithic stirrer reactor (MSR). The purpose of the monolithic stirrer is to mix the reactants, to disperse the gas in the liquid phase, and at the same time to act as catalytic support.[7] The MSR has been proposed for reactions in which the catalyst is suspended in the reaction medium and represents a promising design for gas−liquid heterogeneous catalytic reactions. It was used in hydrogenation reaction with different agitator configurations.[7,8] A similar device was used in biological reactors and in studies comparing the performance of immobilized enzymes.[9] Recently, a study of the gas to liquid mass transfer under different agitation regimes was carried out in a rotating foam reactor where foams were placed in the agitator.[10]

The hydrogenation of edible oils has been carried out industrially since the beginning of the 20th century for increasing the fusion temperature and oxidation resistance.[11] A novel approach is the application of structured catalytic systems.[12,13] Their application would allow one to eliminate some steps of the hydrogenation process, such as filtration steps, catalyst disposal, and other related issues. This could compensate for the higher costs of the catalyst if the operational problems posed by, among other aspects, the possibility of recovery and reuse of the catalyst are solved. The stirred monolith reactor is one of the several reactor design proposed.[12−16] It appears to be a versatile tool, allowing catalyst reuse and operation in a more environmentally benign manner than the conventional oil hydrogenation process. Boger et al.[14] compared the activity of powder and ceramic monolithic catalysts for oil hydrogenation, while Pérez-Cadenas et al.[15,16] used Pd on a carbon monolith to study the hydrogenation of fatty acid methyl esters.

The present work studies the potential use of commercial monolithic systems, in the partial hydrogenation of sunflower oil using a MSR. A commercial cordierite substrate for car exhaust control was modified for the present reaction by

Received: May 26, 2012
Revised: August 2, 2012
Accepted: August 29, 2012
Published: August 29, 2012

ACS Publications © 2012 American Chemical Society

dx.doi.org/10.1021/ie3013727 | *Ind. Eng. Chem. Res.* 2012, 51, 12222−12232

reimpregnating it with a Pd precursor. The objective of the work was to revise the hydrodynamic aspects of the monolithic stirrer reactor and to show the catalytic applicability of this reactor in a heterogeneously catalyzed gas−liquid reaction for viscous liquids, such as vegetable oils. The gas−liquid and liquid−solid mass transfer characteristics of the monolithic stirrer reactor were studied.

2. MATERIALS AND METHODS

2.1. Monolithic Catalyst. Pd/cordierite catalysts were prepared by wet impregnating a commercial cordierite monolith (400 cpsi) used for automobile exhaust control. The monolith alumina washcoating was promoted with CeO_2 and ZrO_2 and also contained small amounts of Pd, Pt, and Rh. The cordierite monolith was cut in order to provide for different shapes of monolith stirrers: a rectangular block (MB), a regular cylinder (C90), and a truncated cylinder (C50). These samples were reimpregnated with aditional Pd for which Pd acetylacetonate [$Pd(C_5H_7O_4)_2$, PdAcAc)] was used as metal precursor. The monoliths were contacted with a toluene solution of PdAcAc at room temperature during 24 h. Following this, they were dried under N_2 flow at 423 K for 2 h and then calcined at 773 K during 2 h.

2.2. Monolithic Catalyst Characterization. The Pd cordierite catalysts were characterized using N_2 adsorption isotherms at −196 °C for surface area measurements (Micromeritics ASAP 2000 system). Catalyst composition was determined by atomic absorption spectroscopy using a GBC AVANTA Σ unit and X-ray fluorescence using a PANalytical MagiX spectrometer with Rh anode, LiF200, PE, PX1, and PX4 crystals under He atmosphere. Scanning electron microscopy (Hitachi model S-2700, 15 kV voltage of acceleration) and transmission electron microscopy (JEOL 100 CS operated at 100 keV) were used for topographical and particle size studies. A conventional ultrasonic method was used for the washcoating adherence test.

2.3. Catalytic Activity Measurements. The catalytic activity tests were carried out in a 0.6 L Parr reactor equipped with a magnetically driven agitator that was modified to perform as a monolithic stirrer. All the reactions were done at 373 K and 413 kPa. Further experimental details on the activity tests procedure are given elsewhere.[12]

The reaction products were analyzed by gas chromatography. Triglycerides (TG) derivatization for further analysis was carried out following the IUPAC 2.301 standard method. Chromatographic analysis were carried out in a HP4890D gas chromatograph using a SUPELCO SP2560 100 m × 0.25 mm × 0.2 mm capillary column. Operating conditions and related procedures following the AOCS Ce 1c-89 norm. The fatty acids in the analyzed samples were identified by comparison with the Supelco 47885-U analytical standard. The iodine index is a measure of TG molecules insaturation. Its value decreases as long as the number of double bonds diminishes and it can be determined from the chromatographic analysis according to norm AOCS Cd 1c-85.

2.4. Flow inside the Monolith Channels. An experimental method based on torque (τ) measurements, proposed by Edvinsson et al.,[6] was used to estimate superficial velocity within the monoliths channels (from eq 4−6). The agitator was directly coupled to a 0.25 HP (Bodine Electric Co.) direct current electric motor. Torque was determined from current and voltage measurements made using two digital multimeters BAW DT 838. Agitation speed was measured with a digital optical tachometer (Schwyz SC114). Experiments were done under three different conditions: (a) using a regular monolith (τ_1), (b) using a monolith with its frontal area sealed with silicone and (c) replacing the monolith with an open cylindrical tube of similar dimensions (τ_0).

2.5. Gas Absorption Measurements: Operation Procedure. To determine the gas to liquid mass transfer coefficient ($k_{GL}a$) a method was used that requires one to measure the pressure variation of the gas phase in the reactor headspace a function of time at a given agitation speed.[10,17,18] The following procedure was adopted:

(1) The liquid was degassed under agitation until an equilibrium pressure is reached.
(2) The agitation was stopped and the system pressurized at P_m = 60 psi.
(3) Agitation was then initiated. Since this favors mass transfer from the gas to the liquid phase, the pressure starts to drop.
(4) Record the pressure as a function of time until a final pressure (P_f) is reached.
(5) Integrate the mass balance between gas and liquid phases between initial and final times and calculate $k_{GL}a$ from eq 8.

The amount of hydrogen incorporated to the liquid phase under the different reaction conditions was determined by measuring the pressure drop and the instantaneous hydrogen flow rate using a Matheson 8270 mass flow controller.

2.6. Evaluation of Diffusional Controls. Carberry-type criteria were used for establishing the presence or absence of gas to liquid and liquid to solid mass transfer resistances. Weisz−Prater criterion was used for estimating intraparticle mass transfer limitations (Table 1).[19]

Table 1. Criteria Used for Analyzing External and Internal Mass Transfer Limitations

mass transfer zone	criterion	equation	condition for nonexistence of limitations
gas−liquid	Carberry	$Ca_{GL} = \frac{r^{obs}}{k_{GL}aC^s_{H_2}}$ (1)	$Ca < 0.05$
liquid−solid	Carberry	$Ca_{LS} = \frac{r^{obs}}{k_{LS}a_mC_i}$ (2)	$Ca < 0.05$
intraparticle	Weisz−Prater	$\Phi_i = \frac{r^{obs}_{cat}\rho_{cat}\delta_C^2}{De_iC_i}$ (3)	$\Phi \ll 1$

The H_2 in the liquid was calculated from Andersson et al.[20] Molecular diffusion coefficients were taken as $D_{H_2} = 2.8 \times 10^{-9}$ m^2/s and $D_{TG} = 6.5 \times 10^{-11}$ m^2/s.[20,21] The density of sunflower oil was 866 kg/m^3, and the viscosity as 7.7×10^{-3} Pa s.[22,23]

To calculate Ca_{LS}, besides reactant properties and geometrical parameters of the monolith, the superficial velocity within the monoliths channels was estimated using the method cited above and it turned out to be 0.16 ms^{-1} at 800 rpm for MB and 0.7 ms^{-1} at 1400 rpm for C90.

3. RESULTS AND DISCUSSION

3.1. Catalyst Preparation. The main physical characteristics of the cordierite monolith are given in Tables 2 and 3 and Figures 1 and 2. Table 4 summarizes Pd loading for samples prepared.

dx.doi.org/10.1021/ie3013727 | Ind. Eng. Chem. Res. 2012, 51, 12222−12232

Table 2. Physical Characteristics of Block and Cylindrically Shaped Monoliths

characteristic	cylindrical monolith C90		block monolith MB	
monolith diameter (m)	D_m	0.017	D_m'	0.031
channel length (m)	L_m	0.016	L_m'	0.023
cell density (cpsi)	n	400	n	400
total number of channels per monolith	n_T	97	n_T'	836
stirrer diameter (m)	D_a	0.057	D_a'	0.049

Table 3. Washcoating and Channels Geometrical Parameters

parameter	value
total wall thickness, δ_w (μm)	165
washcoat thickness, δ_c (μm)	14
washcoat thickness in the corner, a (μm)	80
washcoat radius, R (μm)	159
washcoat density (kg m^{-3})	1574
area/volume ratio, a_m (m^{-1})	2522
empty fraction, ε_m	0.72
hydraulic diameter, d_h (mm)	1.14
tortuosity, ξ	4[a]
porosity, ε	0.5[b]

[a]Fogler and Scott[19] [b]$\varepsilon = \rho_{cat} V_{pore}$.

The specific surface area was 480, 42, and 25 m^2/monolith for MB, C90, and C50, respectively (26.1 m^2/g$_{monolith}$). AAS and XRF analysis revealed that the commercial cordierite sample contained 0.05 wt % Pt, 0.002 wt % Pd, and 0.02 wt % Rh. As usual, the washcoating thickness was a maximum at the corners and a minimun in the channels side. From SEM micrographs these were estimated to be 80 and 14 μm, respectively.

3.2. Flow inside the Monolith Channels. An experimental method based on torque (τ) measurements, proposed by Edvinsson et al.,[6] was used to estimate superficial velocity within the monoliths channels, from the following equations:

$$v = \frac{B}{\mu_A}\frac{\Delta P}{L_m} \tag{4}$$

$$B = \frac{A_a d_h}{28.46} \tag{5}$$

$$\Delta P = \frac{\tau_1 - \tau_0}{(D_a - D_m)\frac{\pi}{4}D_m^2} \tag{6}$$

Figure 3a shows that the reactor with C90 monolithic stirrer requires an intermediate power between that of a closed monolith and that of an empty tube. This indicates that there is flux within the channels. From these power data the linear velocity within the channels was calculated. The resulting velocities are presented in Figure 3b, for two temperatures. For vegetable oil at 298 K, changes in linear velocity as a function of the stirrer rate are slower. If the fluid temperature is increased (at 373K), linear velocity varies significantly with stirrer rate because of the variation in fluid viscosity.

The estimated channel velocity represents an average velocity for the entire monolith. It is expected that in channels closer to the reactor wall, the channel velocity will be higher than in channels closer to the stirrer shaft.

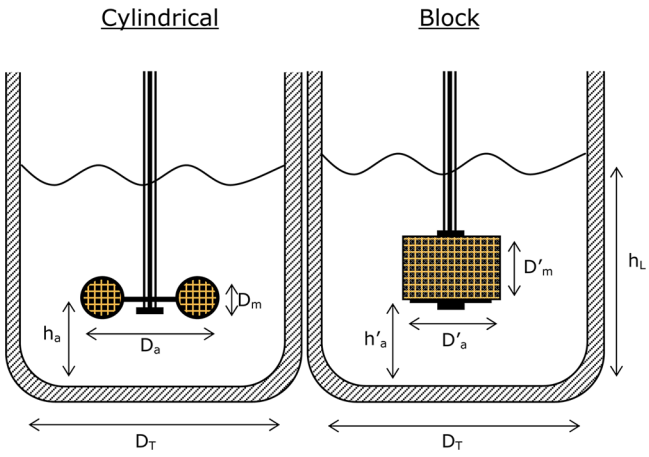

Figure 2. Monolithic agitators' setup.

Table 4. Monolithic Stirrers Pd Loading

sample	palladium loading (wt %)	palladium loading (mg Pd/monolith)
MB-0[a]	0.002	0.4
MB-A	0.007	1.3
MB-B	0.012	2.2
MB-C	0.020	3.6
MB-D	0.025	4.5
C50	0.085	0.8
C90	0.057	0.9

[a]Corresponds to the original monolith.

3.3. Effect of the Dip Tube and the Pressure on the Hydrogen Feed to the System. The amount of gas incorporated into the reaction volume and the rate of its incorporation depend on various factors, i.e., stirrer design, reactor internals, stirrer rpm. The injection of H_2 in the present case is done through a small-diameter dip tube well inside the reactor, and from there it is dispersed in the reacting medium by agitation. Under reaction conditions, H_2 is neither immediately dissolved nor reacted. In this way, once the solubility limit at the reaction temperature and pressure is surpassed the gas will accumulate in the reactor head space and

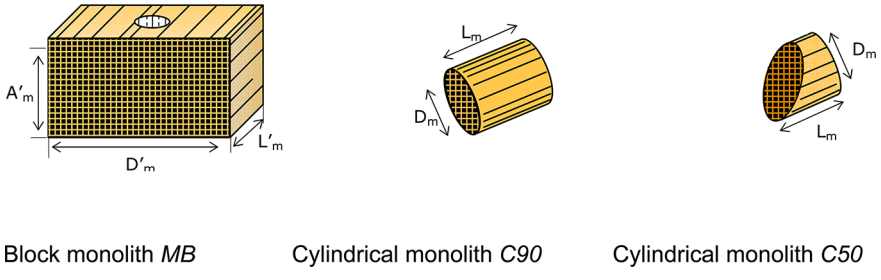

Figure 1. Monolithic stirrer shapes.

dx.doi.org/10.1021/ie3013727 | Ind. Eng. Chem. Res. 2012, 51, 12222−12232

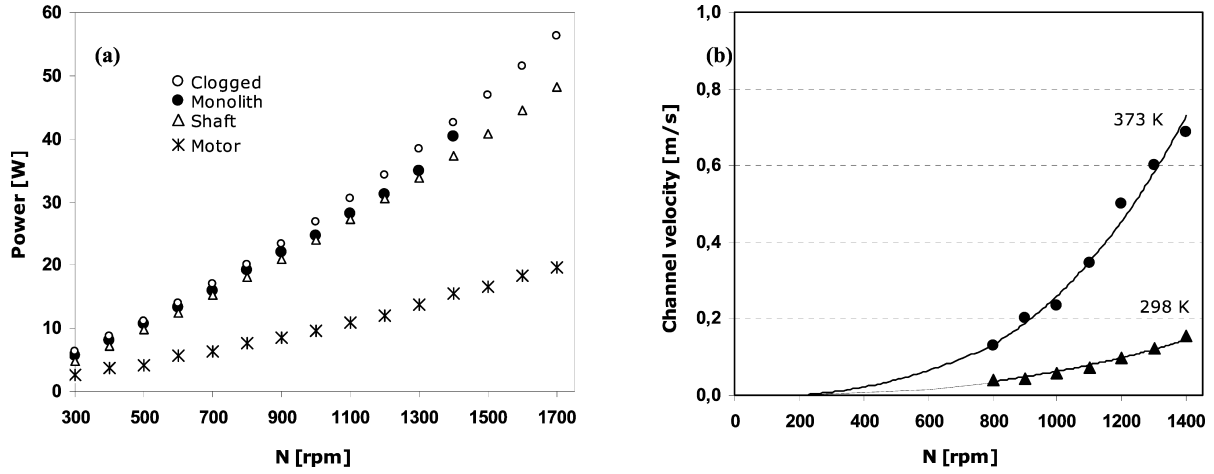

Figure 3. (a) Power as a function of stirrer speed and (b) linear velocity inside the channels as a function of stirrer speed.

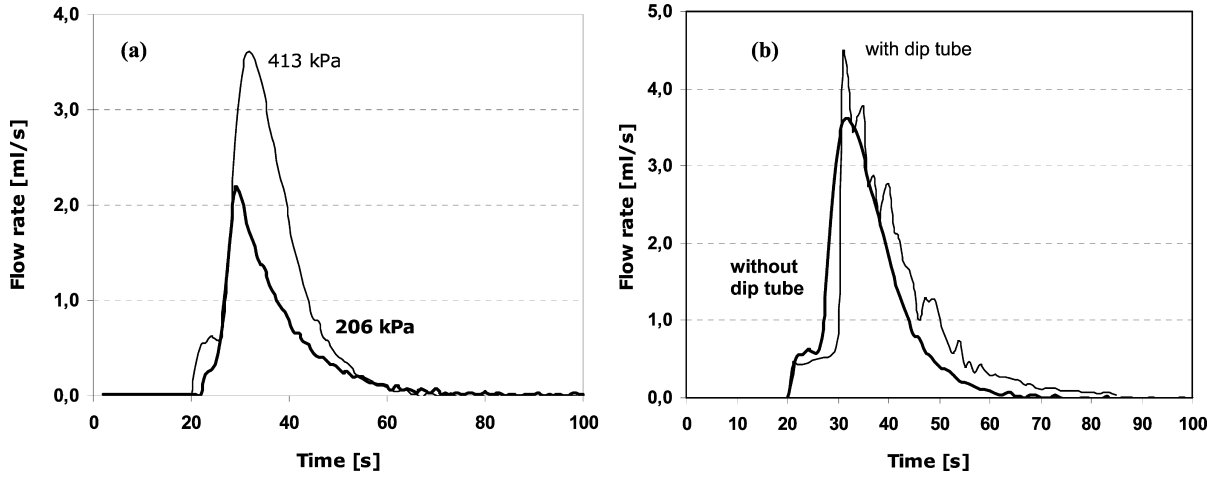

Figure 4. (a) Effect of pressure on hydrogen uptake (C90, N = 1400 rpm). (b) Hydrogen uptake with and without dip tube (C90, N = 1400 rpm, and 413 kPa).

be recirculated by the stirrer into the reaction volume. To determine the influence of this process of feeding H_2 to the reaction, the amount of H_2 incorporated was measured with and without the dip tube and under different operating pressure. Results are presented in Figure 4a,b. It is shown that by using a dip tube 15% more hydrogen is incorporated into the reaction volume.

Changing H_2 pressure in the reactor head space modifies the amount of gas fed to the reaction. At 413 and 206 kPa, 50 and 28 mL of hydrogen were respectively introduced into the reaction volume (See Figure 4a).

3.4. Effect of Agitation Speed on the Hydrogen Feed to the System. In a similar way, the volume of hydrogen incorporated into the reaction was measured at different agitation regimes (800 and 1400 rpm) and for every monolithic stirrer shape, and the results are shown in Table 5. The results for monolith C90 are shown in Figure 5. It can be observed in Figure 5b that the volume of gas incorporated increases strongly with rpm up to 700 rpm. From this point on the gas volume steadily tends to 50 mL. Obviously, the time required for the process is shorter the faster the stirrer rotation.

3.5. Mass Transfer Characteristics. *3.5.1. Gas–Liquid Mass Transfer Coefficient k_{GL}.* In vegetable oil, variation of hydrogenation properties during the reaction progress could alter the value of k_{GL}. During hydrogenation, oil density and viscosity increase, and these changes may slow down the mass transfer, although this is not the case with sunflower oil hydrogenation.[24,25]

Table 5. Total H_2 Volume (VH_2) and Maximum Flow Rate (FR_M) and the Corresponding Time (t_M), for the Monolithic Stirrers

	800 rpm			1400 rpm		
monolithic stirrer	VH_2 (cm^3)	FR_M (cm^3/s)	t_M	VH_2 (cm^3)	FR_M (cm^3/s)	t_M
MB	50.2	1.0	22	50.7	3.6	7
C90	50.4	0.8	51	50.3	3.2	12
C50	50.8	1.1	17	49.6	3.2	6

Several methods exist for k_{GL} estimation in agitated systems. In the present case the procedure proposed by Stenberg and Schöön[26] was used for monolithic stirrer MB, by plotting the reciprocal of the hydrogenation rate versus the inverse of the catalyst mass according to the following equation

$$\frac{C_{H_2}}{-r^0_{H_2}} = \frac{1}{k_{GL}a} + \frac{1}{m}\left(\frac{1}{k_{LS}a_m} + \frac{1}{k\eta}\right) \quad (7)$$

where $r^0_{H_2}$ is the hydrogen consumption rate in the oil hydrogenation reaction.

dx.doi.org/10.1021/ie3013727 | Ind. Eng. Chem. Res. 2012, 51, 12222–12232

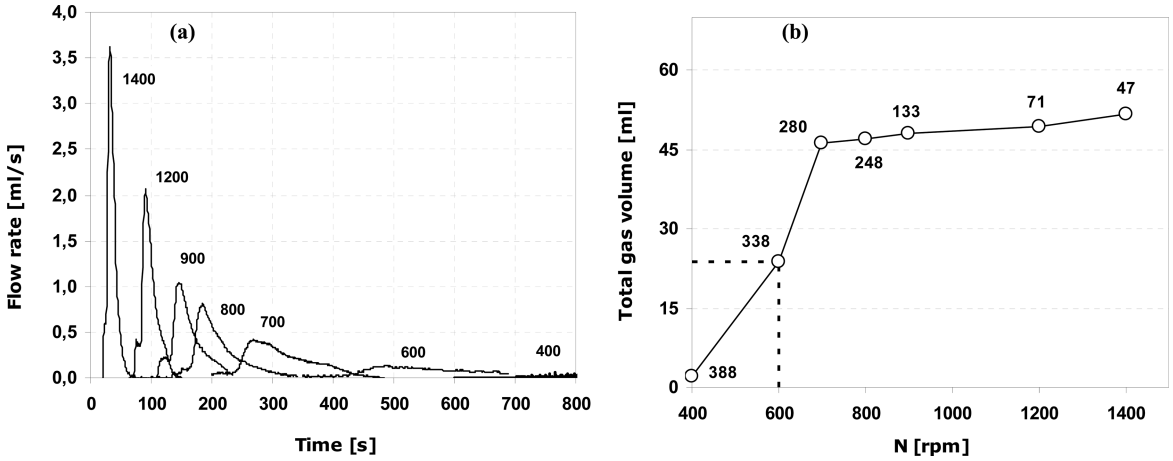

Figure 5. Hydrogen incorporated using monolith C90. (a) Flow rate versus time profile at different agitation regime. The numbers on the curves indicate the value of the stirrer speed (in rpm). (b) Volume of gas incorporated. Mixing time (in seconds) is indicated close to the symbols.

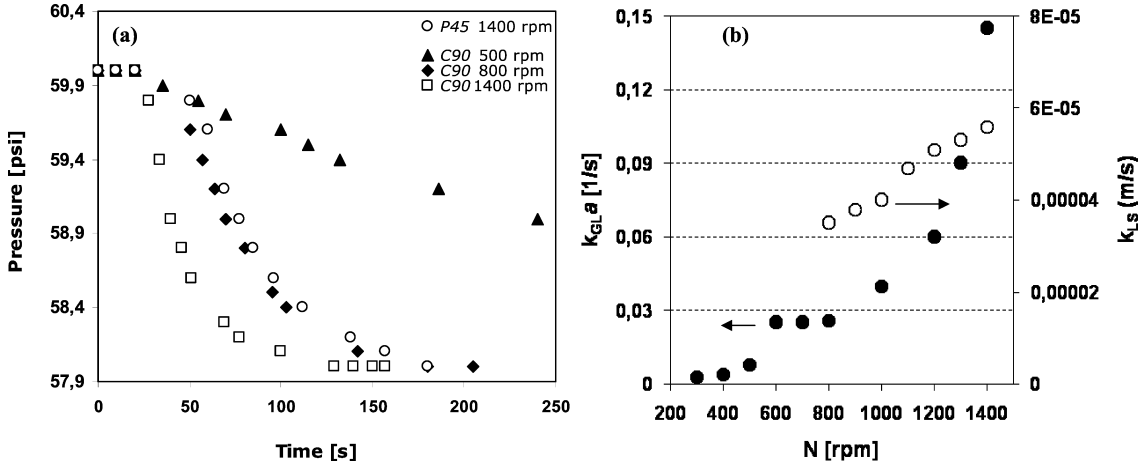

Figure 6. (a) Pressure as a function of time at different stirrer speeds, for C90 and pitched blade turbine (P45). (b) Gas–liquid (for C90 monolith) and liquid–solid mass transfer coefficients as a function of *N*.

In agreement with this equation, the intercept at the *y*-axis is associated with the magnitude of the mass transfer resistance between the gas and the liquid. From experiments on all MB samples, $k_{GL}a$ = 0.12 s^{-1} and $k_{GL}a$ = 0.6 s^{-1} were obtained at 800 and 1400 rpm, respectively.

In the case of monolithic stirrer C90, the method of physical absorption presented by Teramoto et al.[17] was used. In this method, the change in H_2 pressure in the head space with time relates to the gas to liquid mass transfer through the k_{GL} coefficient according with the following equation:

$$\ln\left(\frac{P_{me} - P_f}{P - P_f}\right) = \left(\frac{P_{me} - P_0}{P_f - P_0}\right) k_{GL}a(t - t_0) \tag{8}$$

The results are given in Figure 6a,b. A strong agitation induces a pronounced decrease in pressure, indicating a fast gas transfer to the liquid phase. The pressure stabilizes when the volume of gas transferred is about 50 mL. The mass transfer coefficient k_{GL} increases when the agitation regime increases. An important change is observed when the system reaches the critical velocity at which the vortex is formed (see the discontinuity in Figure 6b). This confirms that the gas transferred corresponds not only to solubilization but also to formation of bubbles.

3.5.2. Liquid–Solid Mass Transfer Coefficient, k_{LS}. Hydrogen and triglycerides mass transfer to the solid surface where the catalyst is located occurs inside the monolith channels. This transport is strongly influenced by the flow pattern that also depends on the phases properties (density, viscosity, and surface tension), the agitation speed, and the channel geometry. The liquid–solid mass transfer coefficient, k_{LS}, must be calculated from correlations relating bubble geometry, length of liquid portion in the channels, and the velocity of the phases.[27] In this work, the Lévêque correlation for liquid solid mass transfer was used[28,29]

$$Sh = 1.16(L_m/d_h Re \times Sc)^{-1/3} \tag{9}$$

for $Gz < 0.05$.

This expression was previously applied for MSR and it is presented in terms of dimensionless numbers useful for k_{LS} estimation.[30,31] Figure 6 shows the data obtained, k_{LS} values, increase with agitation speed. When the latter is higher than 1000 rpm, a stabilization period is observed. In biphasic flows an increase in agitation speed and the linear velocity not necessarily results in an improvement in mass transfer. High speed values may result in the formation of an annular flow that produces a thick film against the wall and a poorer mass transfer in the radial direction.

3.6. Catalyst Activities. Since the commercial monolith characterization analysis indicates the presence of Pt and Rh

dx.doi.org/10.1021/ie3013727 | *Ind. Eng. Chem. Res.* 2012, 51, 12222–12232

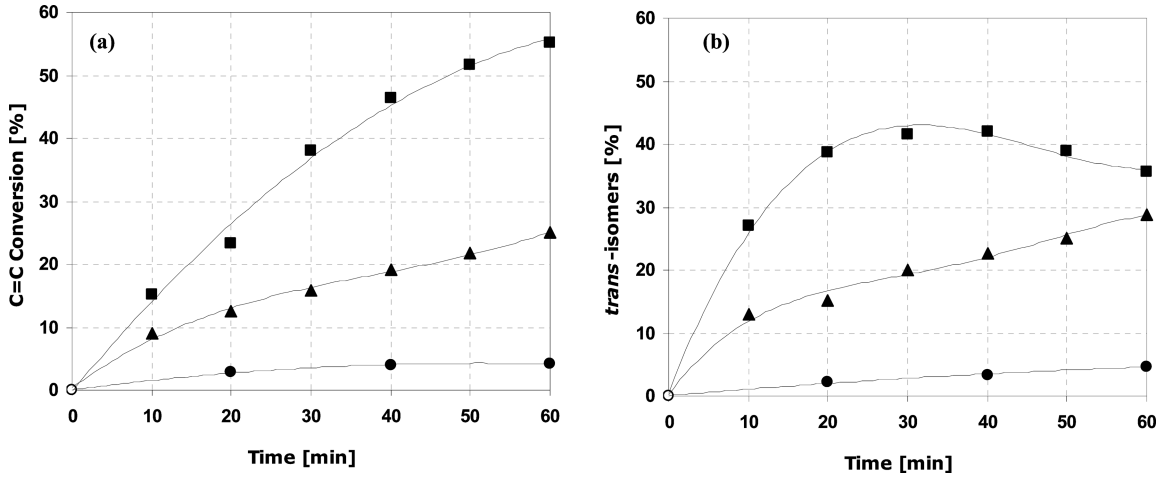

Figure 7. (a) C═C conversion and (b) formation of trans-isomers as a function of time. Catalysts: ●, MB-0; ▲, MB-A; ■, MB-B. Conditions: 250 cm^3, 413 kPa, 373 K, and 800 rpm.

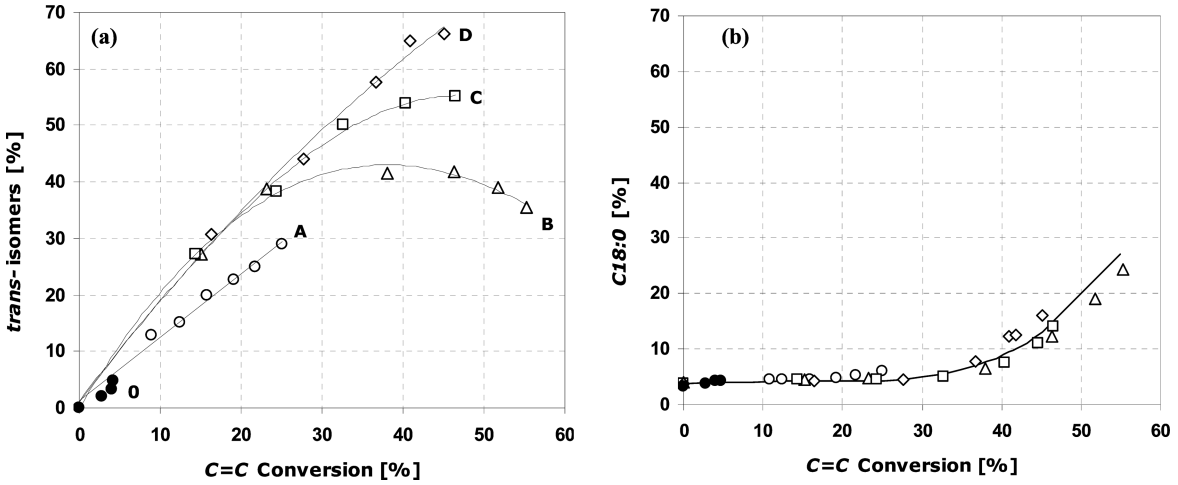

Figure 8. Formation of (a) trans-isomers and (b) C18:0 as a function of the C═C conversion. Catalysts: ●, MB-0; ○, MB-A; Δ, MB-B; □, MB-C; ◇, MB-D. Conditions: 250 cm^3, 413 kPa, 373 K, 60 min, and 800 rpm.

besides Pd, some experiments were run on the hydrogenation of sunflower oil using a block monolithic stirrer having the original commercial metal composition, a sort of blank of the catalyst (MB-0). This monolith was reduced in situ in flowing hydrogen at 404 K during 30 min. The reaction was carried out at 1400 rpm, 413 kPa, and 373 K, and a C═C conversion lower than 5% was found for a reaction time of 120 min.

Activity tests were conducted using block monolithic stirrers with different Pd loading with the purpose of investigating the effect of metal loading. With the exception of the latter, the experimental variables (oil volume, oil properties, reaction temperature, reaction pressure, agitation regime, etc.) were kept constant. The results, given in Figure 7, indicate that the monolithic catalysts are highly active under the selected reaction conditions. The increase in Pd loading is accompanied by an increase in activity and favors the production of trans-isomers.

It is well-known that oil hydrogenation reaction is affected by mass transport limitations. In the presence of the Pd surface, TG molecules will adsorb onto it and will be ready for hydrogenation. Since there are transport limitations, they will stay at the surface long enough to be isomerized instead of hydrogenated due to the lack of sufficient hydrogen. This yields a higher selectivity for isomerization products rather than hydrogenation ones. Due to thermodynamics reasons, trans-isomers are favored. Figure 8a,b present trans-isomers and saturation product formation for block monolithic stirrers as a function of conversion. Data show that, at similar conversion, the higher the metal loading, the higher the selectivity for trans-isomers without a significant increase in saturation products formation. On the contrary, C18:0 levels are similar in all the reactions. This confirms that intermediate reactions prevail over total saturation.

Initially, a set of experiments was done on a series of block monolithic stirrers using similar reaction conditions: 250 mL, 800 rpm, 413 kPa, and 313 K. The information collected was used to calculate the Weisz−Prate modules (Φ) and Carberry numbers (Ca). The results are given in Table 6.

The results indicate that the reaction occurs in a transport limitation regime in which both internal and external mass transport resistances are significant not only for the TG but also for H_2. The latter finds also difficulties in transferring from gas to liquid phase under these operating conditions, as revealed by the Ca_{GL} number. Ca_{LS} numbers for hydrogen around 0.1 seem to indicate that the reaction might be controlled by the transport of this species either because the flow in the channels

dx.doi.org/10.1021/ie3013727 | Ind. Eng. Chem. Res. 2012, 51, 12222−12232

Table 6. Weisz–Prater Modules and Carberry Numbers for Block Monolithic Stirrers Catalysts[a]

sample	Φ_{H_2}	Φ_{TG}	$Ca_{GL\ H_2}$	$Ca_{LS\ H_2}$	$Ca_{LS\ TG}$
MB-A	1.7	0.7	0.56	0.11	≪0.05
MB-B	1.9	0.8	0.83	0.14	≪0.05
MB-C	2.4	1.1	0.84	0.13	≪0.05
MB-D	2.5	1.1	0.86	0.14	≪0.05

[a]Operation conditions: 250 mL_{oil}, 800 rpm, 413 kPa, and 313 K.

is not favored at this agitation regime or because flow occurs preferentially in some channels. A naked-eye analysis of used block monoliths reveal that reaction does not practically use the central portion of the catalyst. According to the low $Ca_{LS\ TG}$, values the triglyceride transfer to the catalyst is not limited.

The effect of the agitation regime on the reaction was studied. Experiments run under two different agitation speeds using a block monolithic stirrer indicate that agitation has important effects on reaction activity and selectivity.

A sample of a block monolithic stirrer (MB-C) was tested for oil hydrogenation under different agitation speeds under similar reaction temperature and pressure than previous experiments. $Ca_{GL\ H_2}$, $Ca_{LS\ H_2}$, and $Ca_{LS\ TG}$ were also calculated. Results are presented in Figure 9.

As can be seen, conversion increases with agitation rate up to 1200 rpm, remaining mostly unchanged since then. $Ca_{GL\ H_2}$ drastically decreases up to 1200 rpm from where it continues to decrease at a slower pace. $Ca_{LS\ H_2}$ presents an opposite trend, initially having a value of 0.07 and increasing to 0.15, which is interpreted as the manifestation of hydrogen transfer control between liquid and solid phases in the channels. The Ca numbers for TG remain fairly low. These results indicate that initially, at low agitation rate, gas to liquid mass transfer resistances predominate. As the agitation regime increases, this limitation decreases but does not disappear, and hydrogen transport between liquids and solid phases diminishes. High velocities do not favor mass transport in the radial direction, limiting hydrogen transfer. As expected, an increase in rpm induces a decrease in trans-isomers while an increment in saturate is observed.

It is important to point out that Ca_{LS} numbers were calculated by assuming that hydrogen concentration within the channels was imposed by hydrogen solubility; however, the high Ca value indicates that this concentration value must be lower. Correlations available in the literature for prediction of flow in the channels generally do not take into consideration possible variations in mass transfer that could be present in biphasic flows. The correlations used here were utilized by other authors for calculations in monolithic systems, and frequently they predict higher mass transfer coefficients than those experimentally measured.[2,31]

Similar experiments were conducted using cylindrical monolithic stirrers (C90). Activity and selectivity at different agitation speeds are presented in Figure 10.

It can be observed that C90 shows better selectivity results for trans-isomer formation than MB at similar reaction conditions and conversion. These differences in selectivity are associated with improved transport of hydrogen and a better distribution of flow among the channels. From these results Weisz–Prater modules and Carberry numbers were calculated. The results are shown in Table 7.

The Weisz–Prater modules higher than 1 suggest a strong internal mass transfer limitation for both reactants. In the case of the TG this is probably associated to its large molecular size as well as the catalyst layer width. For hydrogen, mass transfer restrictions are due to the low concentration of it in the proximity of the catalyst, especially at low agitation regimes. Even when agitation improves hydrogen transfer, internal mass transport resistances do not completely disappear. However, the Φ_{TG}/Φ_{H_2} ratio remains fairly constant. This typical behavior was also observed by Jonker et al.[32] for catalyst particles and Waghmare et al.[33] for a monolithic catalyst.

Regarding external mass transfer in the C90 monolith, the Ca numbers lead us to suppose that gas–liquid limitations are still present but almost disappear when the stirrer rotates at 1700 rpm or more. Within the channels the reaction is mainly limited by hydrogen transfer even at high agitation rate, but this is not the case for triglyceride.

The $Ca_{LS\ H_2}$ decreases as agitation increase. Differently from what it was observed for MB monoliths, when using C90 samples, the increase in agitation speed improves mass transfer

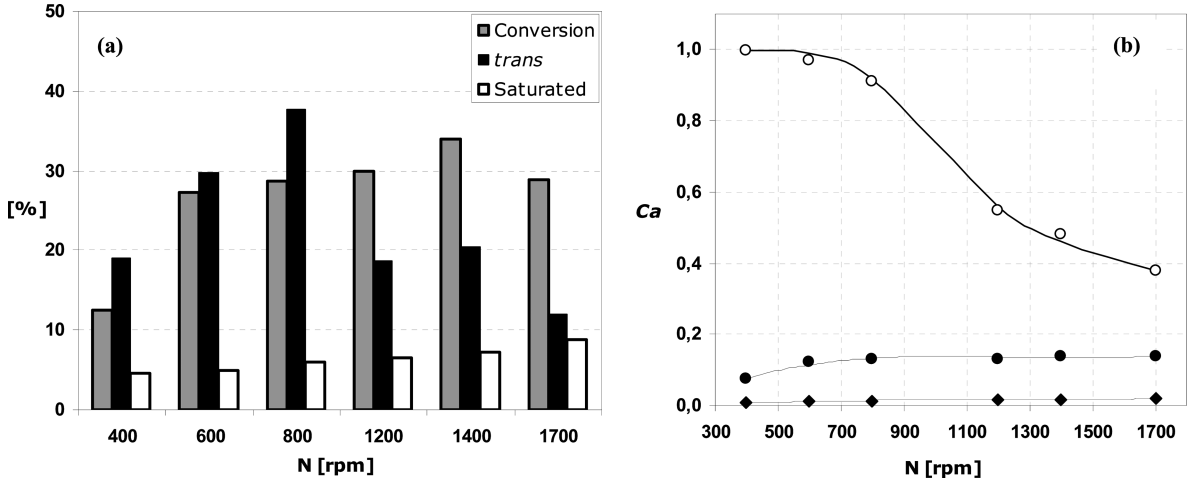

Figure 9. (a) Activity and selectivity in the partial hydrogenation of sunflower oil at 100 °C and 413 kPa with MB-C monolithic catalyst. (b) Carberry number for external mass transfer limitations for the triglyceride: ○, Ca_{GL} for H_2; ●, Ca_{SL} for H_2; ◆, Ca_{SL}. Conditions: 250 cm^3, 413 kPa, 373 K, 30 min, and 800 rpm.

dx.doi.org/10.1021/ie3013727 | Ind. Eng. Chem. Res. 2012, 51, 12222–12232

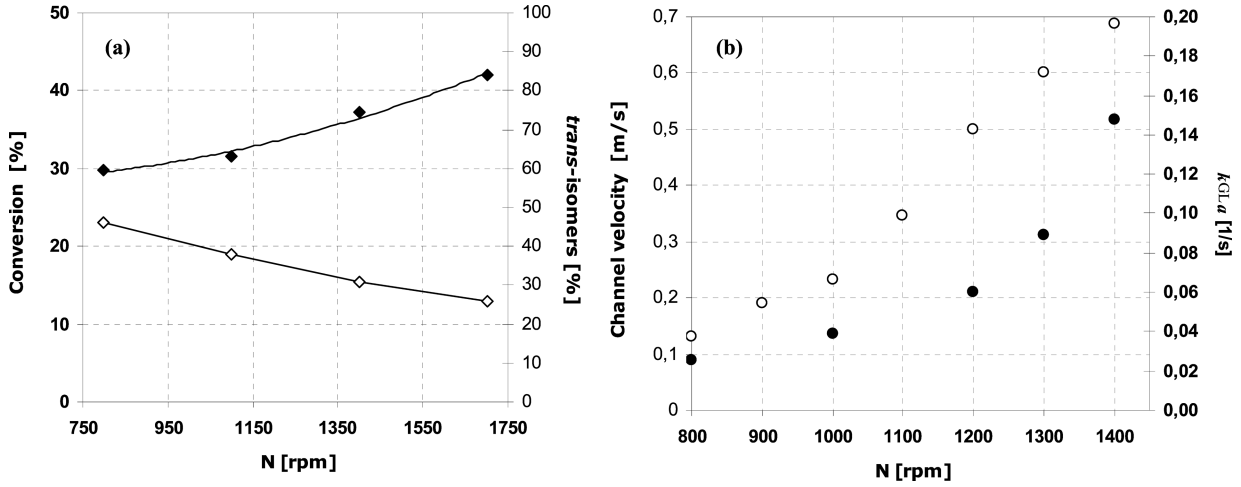

Figure 10. Partial hydrogenation of sunflower oil at 373 K and 413 kPa with C90 monolithic catalyst: (a) (◆) C═C conversion and (◇) trans-isomers formed as function of the stirrer speed. (b) (○) Channel velocity and (●) $k_{GL}a$ for different stirrer speed.

Table 7. Weisz−Prater Modules and Carberry Numbers at Different Agitation Speed for C90 Monolithic Stirrer

agitation speed	Φ_{H_2}	Φ_{TG}	$Ca_{GL\ H_2}$	$Ca_{LS\ H_2}$	$Ca_{LS\ TG}$
800	10	4.4	1.00	0.80	≪0.05
1100	11	4.7	1.00	0.60	≪0.05
1400	12	5.5	0.54	0.60	≪0.05
1700	15	6.8	0.08	0.50	≪0.05

within the channels, as evidenced by the Ca numbers. This is probably due to an improvement in flow in the channels along with short channels that do not allow the flow to achieve a fully developed pattern.

Even though high rpm regimes are desirable if high mass transfer is required, these severe conditions induce structural damages to the monolith. Vibrations and prolonged exposure to hot oil weaken the monolith. Data in this regard will be provided in the near future.

Experiments with cylindrical monolithic stirrers C50 showed good activity and selectivity results, but mechanical failures of the monolith produced severe damage that did not allow further studies.

3.7. Study of the Stability of the Catalyst. The possibility of catalyst reuse is one of the most important issues in monolithic catalyst development, since it could result in lower preparation, reposition, and disposal costs together with the possibility of process simplification by elimination of some filtering and whitening steps on it. Therefore, an adequate monolithic catalyst should be the one that can be used several times before regeneration or replacement is required. In order to evaluate activity, selectivity, and mechanical performance of the monolithic catalyst, several consecutive hydrogenation reaction were carried out using a single sample of a block monolith (MB-B; MB-C) without intermediate treatment between reactions. Results are presented in Figure 11. It can be seen that activity decays between reactions in a similar way in both samples, although it is more pronounced in sample MB-B. Boger et al.[14] observed similar behavior using palladium-based monoliths.

Figure 12 summarizes the relative activity data as a function of the number of consecutive uses. It is clear that even though the activity decreases continuously without reaching a constant value, the monolith can be used up to five times before losing 50% of its original activity.

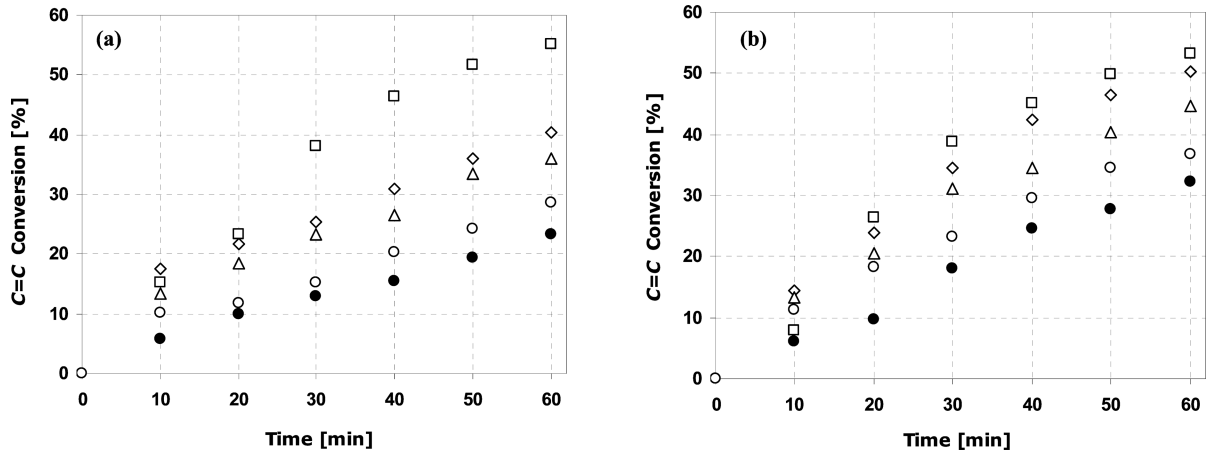

Figure 11. C═C conversion as a function of time in the partial hydrogenation of sunflower oil for five consecutive reactions with (a) MB-B and (b) MB-C catalysts. Conditions: 373 K, 413 kPa, 250 cm^3, 30 min, and 800 rpm. Reactions: □, first; ◇, second; Δ, third; ○, fourth; ●, fifth.

dx.doi.org/10.1021/ie3013727 | Ind. Eng. Chem. Res. 2012, 51, 12222−12232

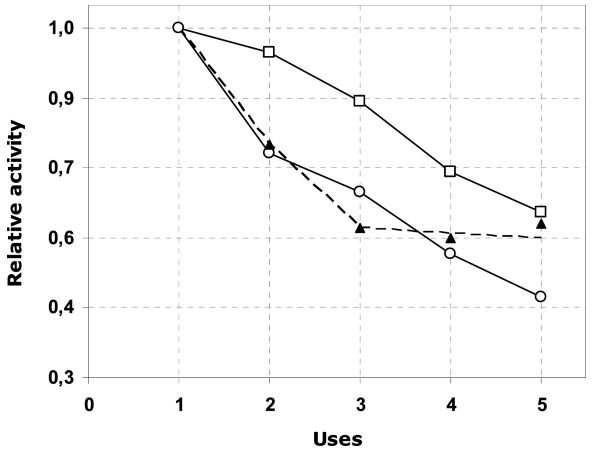

Figure 12. Relative activity for consecutive reactions with MB catalyst in comparison with literature data: ○, MB-B; □, MB-C; ▲, Boger et al.[22]

Results in terms of product distribution are given in Figure 13. Selectivity is similar to that of other MB samples. Some differences are observed for samples used in this experiment. They are associated with the higher Pd loading of sample MB-C. Changes in selectivity for saturated products between the first and second uses are related to the higher activity for the first use together with a poorer hydrogen feed.

The activity loss could be the result of poisoning by strong adsorption of oil impurities, structural damage to the monolithic catalyst, or physical blockage of surface sites by hydrogenated oils. If the latter is the reason, a washing procedure using an appropriate solvent and temperature or a controlled combustion process could be enough for catalyst regeneration. With this purpose in mind, a washing procedure using hexane at 333 K during 45 min and a controlled calcination (2 K/min up to 673 K) were implemented. After these treatments and prior to hydrogenation reaction the catalysts were reduced in flowing hydrogen at 373 K during 30 min.

Using block monolith stirrer samples MB-B, MB-C, and MB-D, a sequence of hydrogenation reactions with intermediate washing or calcination treatments was done. All reactions were done at 373 K, 413 kPa, and 800 rpm and used 250 mL of sunflower oil. The sequence of reactions and regeneration steps were as follows:

MB-B: five reactions → washing → three reactions → washing → three reactions.
MB-C: five reactions → washing → three reactions → washing and calcination → two reactions.
MB-D: three reactions → washing → one reaction → washing → one reaction → washing → one reaction.

The results, for MB-B and MB-C, in terms of relative activity as a function of the number of uses are presented in Figure 14.

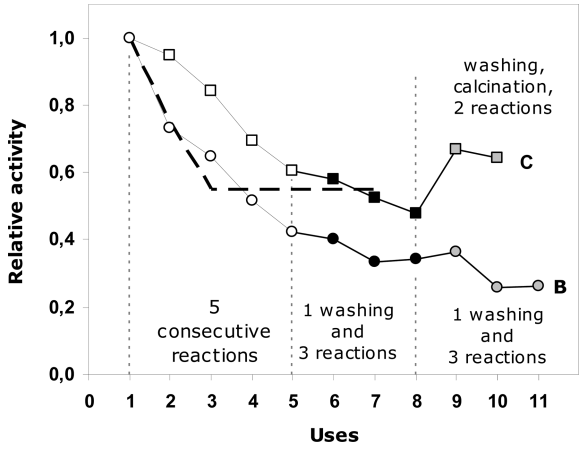

Figure 14. Relative activity as a function of number of uses for MB catalysts: □, MB-B; ○, MB-C; – –, Boger et al.[22] Conditions: 373 K, 413 kPa, 60 min, 250 cm^3, and 800 rpm.

For samples MB-B and MB-C, the activity loss is partially controlled by the washing treatment. This is clearly evident for MB-B sample, in which the washing procedure produces a recovery of activity to the level of the previous reaction, although it cannot prevent the continuity of the activity decay. Boger et al.[14] reported similar data for consecutive reactions without intermediate treatments. Incomplete characterization of used monoliths prevents further comparison. For the MB-C sample, however, calcination allows a partial recovery of the activity to the level shown five reactions back in time.

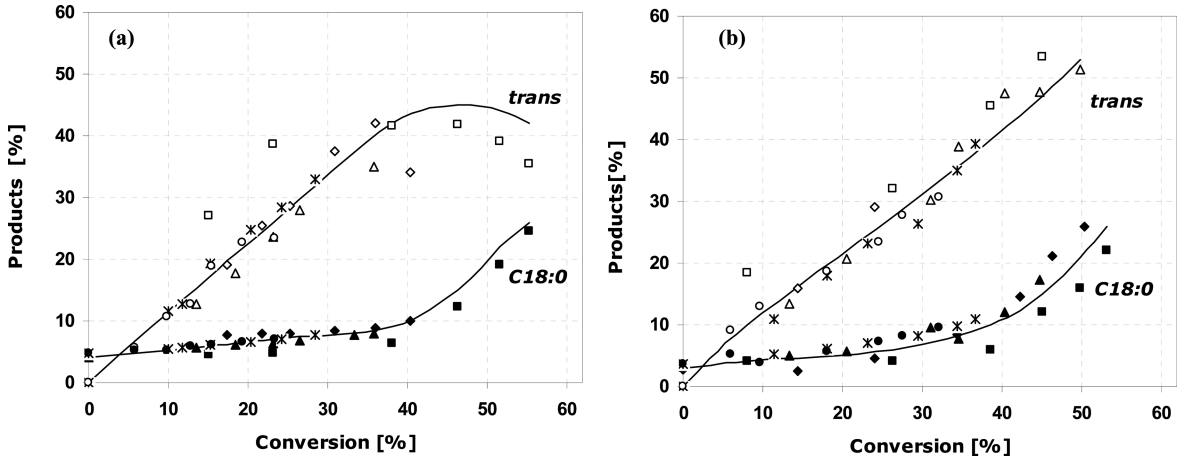

Figure 13. Trans-isomers and C18:0 formed as a function of the conversion in the partial hydrogenation of sunflower oil for five consecutive reactions with (a) MB-B and (b) MB-C catalysts. Conditions: 373 K, 413 kPa, 250 cm^3, and 800 rpm. Reactions: □, first; ◇, second; Δ, third; *, fourth; ○, fifth.

dx.doi.org/10.1021/ie3013727 | Ind. Eng. Chem. Res. 2012, 51, 12222−12232

According to Figure 15, the sequence of three consecutive reactions followed by cycles of reaction−washing used with

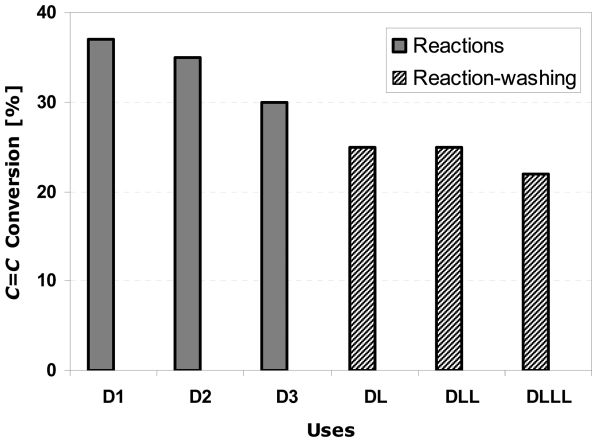

Figure 15. Variations in the activity for the sequence of reaction−washing using MB-D catalyst. Conditions: 373 K, 413 kPa, 30 min, and 800 rpm.

sample MB-D seems to lead to a leveling point in the activity decay similar to the other cases.

The product distribution of the reactions where intermediate treatments between activity tests were used is presented in Figure 16. A moderate change is observed between the first use

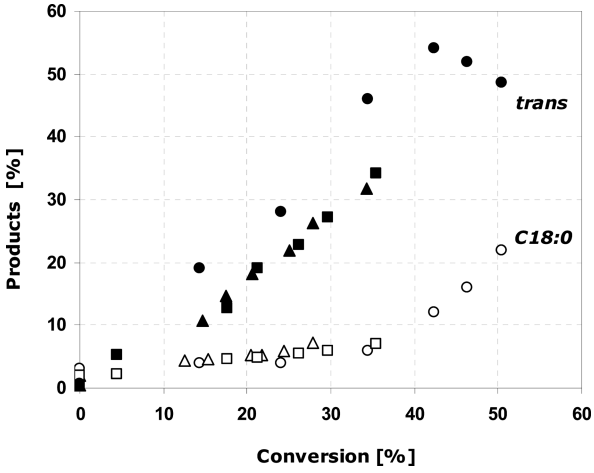

Figure 16. Trans-isomers and C18:0 formed as a function of the conversion for the sequence: ○, MB-C (reaction); Δ, MB-C (washing−reaction); □, MB-C (washing−calcination−reaction).

and the remaining ones for trans-isomers attributed to the higher activity of the initial catalysts. After washing and calcination steps, the product distribution remains almost unchanged. This is evidence that the catalytic surface was not affected in the process.

The rest of the monolithic stirrers made of cylindrical shape were also tested for reuse. They showed a similar activity decay as the one already presented for block monoliths. However, for these geometries catalyst lost due to attrition is more evident than in previous cases and it is particularly severe for C50 monoliths.

4. CONCLUSIONS

The monoliths used in the present paper represent a rapid source of substrates covered with a high surface area support useful for exploratory studies. Their preparation is relatively simple.

The present work shows that the principle of a monolithic stirrer reactor concept works in a heterogeneously catalyzed gas−liquid reaction for viscous liquids, such as vegetable oils.

For the geometry and size of the used reactor, the hydrogen uptake in the oil appears to be independent of the H_2 bubbling system. The maximum volume of hydrogen incorporated into the reaction was similar for all the monolithic stirrer studied, but C90 needed a greater time due to its less efficient agitation regime. The time required for the process is shorter the faster the stirrer rotation.

The volumetric gas−liquid and liquid−solid mass transfer coefficients were calculated at the operation condition and different stirrer rate. The mass transfer coefficient k_{GL} increases when agitation regime increases ($k_{GL}{}^{1400\ rpm} = 5.6k_{GL}{}^{800}$). An important change is observed when the system reaches the critical velocity at which the vortex is formed. On the other hand, k_{LS} values increase weakly with agitation speed ($k_{LS}{}^{1400\ rpm} = 1.6k_{LS}{}^{800}$).

When catalyst activities were analyzed, it was found that the increase in Pd loading is accompanied by an increase in activity and favors the production of trans-isomers. At similar conversion, the higher the metal loading, the higher the selectivity for trans-isomers without a significant increase in saturation products formation. The determination of Weisz−Prate module and Carberry numbers indicate that the reaction occurs in a transport limitation regime in which both internal and external mass transport resistances are significant not only for the triglycerides but also for hydrogen. However, notable improvement are observed: for MB, conversion increases with agitation speed up to 1200 rpm, remaining mostly unchanged since then (similar behavior as k_{LS}), and Ca_{GL} drastically decreases up to 1200 rpm, from where it continues to decrease at a slower pace, in the same way as trans-isomer formation does.

C90 cylindrical monolithic showed the best general performance. Palladium in the central portion of MB block monoliths was not practically used (low channel velocity). C50 monolithic stirrers showed good activity and selectivity but presented mechanical failures.

Study of the stability of the catalyst showed that, even though the activity decreases continuously without reaching a constant value, the monolith can be used up to five times before losing 50% of its original activity. Washing and calcination treatments allows a partial recovery of the activity.

■ AUTHOR INFORMATION

Corresponding Author

*Tel: +54 291 4861700. Fax: +54 291 4861600. E-mail: gtonetto@plapiqui.edu.ar.

Notes

The authors declare no competing financial interest.

■ ACKNOWLEDGMENTS

Authors thank the Universidad Nacional del Sur (UNS) and the Consejo Nacional de Investigaciones Científicas y Técnicas (CONICET) for their financial support.

ABBREVIATIONS

A_a: open frontal area
a_m: geometrical surface area of monolith (m^2 m^{-3})
B: permeability coefficient of monolith (m^2)
C_{H_2}: concentration of hydrogen (mol m^{-3})
d_h: hydraulic channel diameter (m)
k: reaction constant
$k_{GL}a$: volumetric gas−liquid mass transfer coefficient (s^{-1})
k_{LS}: liquid to solid mass transfer coefficient (m s^{-1})
m: mass of catalyst (kg)
N: stirrer rat (rpm)
P: pressure (psi)
t: time (s)
v: linear velocity in monolith channel (m s^{-1})

Sub- and Superscripts

f: final
me: measured
0: initial
TG: triglyceride

Greek Letters

ρ: density (kg m^{-3})
Φ: Weisz−Prater criterion
η: effectiveness factor
τ: torque on stirrer shaft (N m)
μ: viscosity (Pa s)

Adimensional Numbers

$Gz = L/d_h Re \times Sc$
$Re_c = \rho_A V d_c/\mu_A$
$Sc = \mu_A/\rho_A D_i$
$Sh = k_{LS} d_c/D_i$

REFERENCES

(1) Boger, T.; Heibel, A.; Sorensen, C. Monolithic catalysts for the chemical industry. *Ind. Eng. Chem. Res.* **2004**, *43*, 4602−4611.
(2) Waghmare, Y.; Bussard, A.; Forest, R.; Knopf, F.; Dooley, K. Partial hydrogenation of soybean oil in a piston oscillating monolith reactor. *Ind. Eng. Chem. Res.* **2010**, *49*, 6323−6331.
(3) Carberry, J. Designing laboratory catalytic reactors. *Ind. Eng. Chem* **1964**, *56*, 39−46.
(4) Kolaczkowski, S.; , Process for the production of organosilicon compounds. European Patent 0 605 143 A2. 1994.
(5) Bennett, C.; Kolaczkowski, S.; Thomas, W. Determination of heterogeneous reaction kinetics and reaction rates under mass transfer controlled conditions for a monolith reactor. *Trans. Inst. Chem. Eng.* **1991**, *69B*, 209−220.
(6) Edvinsson, A.; Houterman, M.; Vergunst, Th.; Grolman, E.; Moulijn, J. Novel monolithic stirred reactor. *AIChE J.* **1998**, *44*, 2459−2464.
(7) Hoek, I.; Nijhuis, T.; Stankiewicza, A.; Moulijn, J. Performance of the monolithic stirrer reactor: Applicability in multi-phase processes. *Chem. Eng. Sci.* **2004**, *59*, 4975−4981.
(8) Irandoust, S.; Andersen, B. Mass transfer and liquid-phase reactions in a segmented two-phase flow monolithic catalyst reactor. *Chem. Eng. Sci.* **1988**, *43*, 1983−1988.
(9) de Lathouder, K.; Marques Fló, T.; Kapteijn, F.; Moulijn, J. A novel structured bioreactor: Development of a monolithic stirrer reactor with immobilized lipase. *Catal. Today* **2005**, *105*, 443−447.
(10) Tschentscher, R.; Nijhuis, T.; van der Schaaf, J.; Kuster, B.; Schoute, J. Gas−liquid mass transfer in rotating solid foam reactors. *Chem. Eng. Sci.* **2010**, *65*, 472−479.
(11) Fernández, M.; Tonetto, G.; Crapiste, G.; Damiani, D. Revisiting the hydrogenation of sunflower oil over a Ni catalyst. *J. Food Eng.* **2007**, *82*, 199−208.
(12) Sánchez, M., J.; Boldrini, D.; Tonetto, G.; Damiani, D. Palladium catalyst on anodized aluminum monoliths for the partial hydrogenation of vegetable oil. *Chem. Eng. J.* **2011**, *187*, 355−361.
(13) Sanchez, M., J.; Gonzalez Bello, O.; Montes, M.; Tonetto, G.; Damiani, D. Pd/Al_2O_3-cordierite and Pd/Al_2O_3-Fecralloy monolithic catalysts for the hydrogenation of sunflower oil. *Catal. Commun.* **2009**, *10*, 1446−1447.
(14) Boger, T.; Zieverink, M.; Kreutzer, M.; Kapteijn, F.; Moulijn, J.; Addiego, W. Monolithic catalysts as an alternative to slurry systems: Hydrogenation of edible oil. *Ind. Eng. Chem. Res.* **2004**, *43*, 2337−2344.
(15) Pérez-Cadenas, A.; Zieverink, M.; Kapteijn, F.; Moulijn, A. Selective hydrogenation of fatty acid methyl esters on palladium catalysts supported on carbon-coated monoliths. *Carbon* **2006**, *44*, 173−176.
(16) Pérez-Cadenas, A.; Zieverink, M.; Kapteijn, F.; Moulijn, J. Selective hydrogenation of fatty acid methyl esters over palladium on carbon-based monoliths: Structural control of activity and selectivity. *Catal. Today* **2007**, *128*, 13−17.
(17) Teramoto, M.; Tai, S.; Nishii, K.; Teranishi, H. Effects of pressure on liquid-phase mass transfer coefficients. *Chem. Eng. J.* **1974**, *8*, 223−226.
(18) Dietrich, E.; Mathieu, C.; Delmas, H.; Jenck, J. Raney-nickel catalyzed hydrogenations: Gas−liquid mass transfer in gas-induced stirred slurry reactors. *Chem. Eng. Sci.* **1992**, *47*, 3597−3604.
(19) Fogler, H.; Scott, L. *Elements of Chemical Reaction Engineering*, 3rd ed.; Prentice Hall: New York, 1999.
(20) Andersson, K.; Hell, M.; Löwendahl, L.; Schöön, N.-H. Diffusivities of hydrogen and glyceryl trioleate in cottonseed oil at elevated temperature. *J. Am. Oil Chem. Soc.* **1974**, *51*, 171−173.
(21) Fillion, B.; Morsi, B. I. Gas−liquid mass-transfer and hydrodynamic parameters in a soybean oil hydrogenation process under industrial conditions. *Ind. Eng. Chem. Res.* **2000**, *39*, 2157−2168.
(22) Bailey's Industrial Oil and Fat Products, 4th ed.; Swern, D., Ed.; Wiley-Interscience: New York, 1982; Volume *2*.
(23) Noureddini, H.; Teoh, B.; Clements, L. Viscosities of vegetable oils and fatty acids. *J. Am. Oil Chem. Soc.* **1992**, *69*, 1189−1191.
(24) Zieverink, M.; Kreutzer, M.; Kapteijn, F.; Moulijn, J. Gas−liquid mass transfer in benchscale stirred tanksfluid properties and critical impeller speed for gas induction. *Ind. Eng. Chem. Res.* **2006**, *45*, 4574−4581.
(25) Topallar, H.; Bayrak, Y.; Iscan, M. Effect of hydrogenation on density and viscosity of. sunflowerseed oil. *J. Am. Oil Chem. Soc.* **1995**, *72*, 1519−1522.
(26) Stenberg, O.; Schöön, N. Aspects of the graphical determination of the volumetric mass-transfer coefficient (kLa) in liquid-phase hydrogenation in a slurry reactor. *Chem. Eng. Sci.* **1985**, *40*, 2311−2319.
(27) Kreutzer, M.; Du, P.; Heiszwolf, J.; Kapteijn, F.; Moulijn, J. Mass transfer characteristics of three-phase monolith reactors. *Chem. Eng. Sci.* **2001**, *56*, 6015−6023.
(28) Martin, H. The generalized Lévêque equation and its practical use for the prediction of heat and mass transfer rates from pressure drop. *Chem. Eng. Sci.* **2002**, *57*, 3217−3223.
(29) Irandoust, S.; Andersson, B. Monolithic catalysts for non-automobile applications. *Catal. Rev.−Sci. Eng.* **1998**, *30*, 341−392.
(30) De Lathouder, K.; Bakker, J.; Kreutzer, M.; Wallin, S.; Kapteijn, F.; Moulijn, J. Structured reactors for enzyme immobilization: A monolithic stirrer reactor for application in organic media. *Chem. Eng. Res. Des.* **2006**, *84*, 390−398.
(31) Hoek, I.; Towards the catalytic application of a monolithic stirrer reactor. Ph.D. Thesis, Technische Universiteit Delft, 2004.
(32) Jonker, G.; Hydrogenation of edible oils and fats. Ph.D. Thesis, Groningen University. 1999.
(33) Waghmare, Y.; Bussard, A.; Forest, R.; Knopf, F.; Dooley, K. Partial hydrogenation of soybean oil in a piston oscillating monolith reactor. *Ind. Eng. Chem. Res.* **2010**, *49*, 6323−6331.